Reflective cracking retardation using geosynthetic Interlayer: A finite element model study

Nithin Sudarsanan
Joint PhD Scholar, Swinburne University of Technology, Victoria, Melbourne, Australia & Indian Institute of Technology Madras, Chennai, India (nsudarsanan@swin.edu.au)

Prashanthi Putchakayala

Indian Institute of Technology Madras, Chennai, India (prashanthi.putchakayala99@gmail.com)

Rajagopal Karpurapu

Indian Institute of Technology Madras, Chennai, India (gopalkr@iitm.ac.in)

Veeraragavan Amirthalingam

Indian Institute of Technology Madras, Chennai, India (aveeraragavan@gmail.com)

ABSTRACT: Reflective cracking is one of the major distresses found on newly laid overlays. Several rehabilitation techniques have been introduced to reduce the effect of reflective cracking. Commonly used method of surface treatment is by the introduction of interlayer systems. Geosynthetic interlayer system is most effective due to its ease of installation and improvement in service life making it superior to the other interlayer systems. The geosynthetic mechanism to retard the reflective cracking is not completely understood due to its complexity. The finite element model package, ABAQUS, is employed to study the initiation and propagation of crack through the hot mix asphalt. The finite element algorithm written in ABAQUS, called eXtended Finite Element Method (XFEM) is found to be an effective solution and user friendly. Hence, in the present study, a single edge notched beam test is modelled using XFEM for simulating the crack propagation mechanism along with all the other required material parameters for numerical modelling. The HMA beam is analysed as a visco-elastic material as it is more realistic to the field behavior. Based on the basic tensile properties of natural geotextiles like coir and jute, the effect of these materials in reducing reflective cracking has been analysed. The results show that there is an improvement in the crack retardation due to the incorporation of geosynthetic interlayer system.

Keywords: Reflective cracking, Natural Geosynthetics, Numerical Modelling, Crack propagation, ABAQUS, eXtended Finite Element Method (XFEM)

1. INTRODUCTION

One of the major problems faced by practicing highway engineers is rehabilitating the existing deteriorated pavement. Resurfacing the existing pavement with Hot Mix Asphalt (HMA) overlay is frequently adopted because of its inexpensive nature compared to the most Portland Cement Concrete (PCC) rehabilitation alternatives (Bennert, 2009). In addition to the existing discontinuities like joint and cracks in the old pavement, repetitive traffic loading and temperature changes lead to large stresses at the bottom of the HMA overlay. The developed stresses in the overlay lead to the propagation of the existing cracks to the surface of the new overlay which is called "Reflective Cracking".

The tensile and bending stresses which results in this kind of distress can be controlled by the introduction of tensile member at the bottom of the overlay. Various techniques have been

developed over the past several years to control reflective cracking, out of all, interlayer system is found to be the most efficient. For several years, bitumen coated geosynthetic layers have been used as interlayer systems to mitigate reflective cracking. The tensile modulus of these reinforcing systems plays a crucial role in reducing the tensile stresses that develop at the bottom of the HMA overlay. In addition to controlling the reflective cracking, asphalt impregnated geosynthetics also help in reducing the surface water infiltration into the old pavements and thus reducing the associated damage (Button, and Lytton, 2007). Experimental studies and numerical studies have proven that, inclusion of geosynthetic materials in HMA overlay increases the life of the pavements (Baek, 2010; Baek, and Al-Qadi, 2006; Khodaii et al., 2009). Some of the applications have shown little or no impact on retarding reflective cracking due to lack of understanding of the mechanism of interlayer system or as a result of inappropriate installation. Some studies also revealed that the use of synthetic material is not economical (Baek, 2010; De Bondt, 1999; Nithin et al., 2015).

In the present study, two natural geotextiles made of Coir and Jute are chosen to study the efficiency in the mitigation of the reflective cracking. In spite of having good mechanical properties, the potential use of natural geotextiles as paving fabrics is not explored sufficiently. But these natural geosynthetics are believed to have high strength at low strains and reasonable value of melting point which are the main requirements of paving fabrics. Use of natural geosynthetic materials is believed to give an economical solution compared to the use of synthetic materials (Nithin et al., 2014). Numerical modelling or Finite element analysis gives an insight into mechanism of crack initiation and crack propagation. Numerical modelling along with experimental studies lead to greater understanding about the mechanism of reflective cracking. Taking the above advantages into account, the effect of natural geosynthetics in mitigating the reflective cracking is being studied using fracture mechanics based finite element analysis by the simulation of a single edge notched beam test. The model of three-point beam bending is developed with and without geotextile reinforcement to see the trend in the improvement in the strength and the control in the crack propagation.

2. MATERIAL CHARACTERISATION FOR NUMERICAL MODELLING

Numerical analysis requires the proper understanding of constitutive modelling of materials and various methods used to model the crack propagation. In the present modelling, materials used are Asphalt concrete and Geosynthetics. Their material properties are of utmost importance and whose determination is explained. Interface and its properties between HMA and geosynthetic materials plays a vital role in the modelling. The calculation of interface properties is also discussed in the paper. The fracture properties of HMA determines the character of the crack propagation. Main property of geosynthetic material is tensile strength and is found using wide width tensile strength tests. Following sections describe the required parameters and models for numerical modelling of three-point beam bending test.

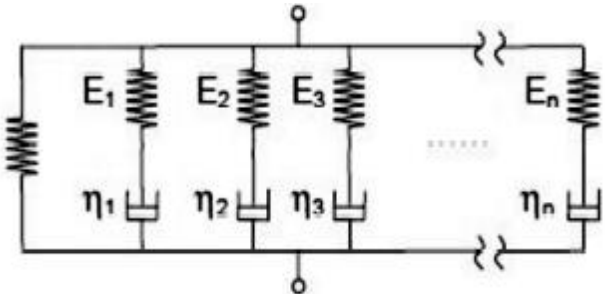

Figure 1. Generalized Maxwell solid model (Baek, 2010)

2.1 Linear Viscoelastic model for Asphalt concrete

It is essential to use appropriate constitutive models to capture the actual behaviour of the material. Among different materials in this study, HMA is the key material. HMA is a visco-elastic material for which the relationship between stress and strain depends on time and temperature. HMA is assumed to be linear viscoelastic for which, there is a linear relationship between stress and strain at any time. Constitutive models for visco-elastic materials are derived by considering linear elastic springs and dashpots. An improvisation in the models lead to Generalized Maxwell's model (Kim, 2009). Generalised Maxwell model consists of several Maxwell units connected in parallel as shown in Figure 1.

Constitutive law for an isotropic linear viscoelastic material is defined as an integration of shear and bulk modulus parts with respect to time as shown in Equation 1 (Christensen, 2012).

$$\sigma(t) = \int_0^t 2G(t-t')e'dt' + \int_0^t K(t-t')\Phi'dt' \tag{1}$$

Where G(t) and K(t) are shear and bulk moduli with respect to relaxation time t′, ε′ and ϕ′ are mechanical deviatoric strain and volumetric strain respectively. G(t) and K(t) are defined using Prony parameters as shown in Equation 2 & 3.

$$G_R(t) = G_0\left[1-\sum_{i=1}^{n} g_i\left(1-e^{-t/t_i}\right)\right] \tag{2}$$

$$K_R(t) = K_0\left[1-\sum_{i=1}^{n} k_i\left(1-e^{-t/t_i}\right)\right] \tag{3}$$

Where g_i, k_i and N are the Prony parameters. Prony series is used to describe a wide range of viscoelastic material behaviour. These Prony parameters indirectly represent the properties of linear springs and dashpots used in the mechanical models like Generalized Maxwell model. Prony parameters are determined by using the dynamic modulus test. Dynamic modulus test is used to determine the complex modulus (E^*) and phase angles at various temperatures and frequencies. A master curve is built to shift the whole experimental data to a reference temperature with respect to a loading frequency based on AASHTO guidelines. The shear complex modulus $|G^*|$ was calculated from $|E^*|$ using a simple relationship of G(t)=E(t)/2(1+μ) under an assumption that HMA is an isotropic material. Bulk modulus $|K^*|$ was also calculated from the basic relationship. A constant value of 0.2 was assumed for Poisson's ratio as no measurement was available to characterize the time and temperature dependent μ. The shear complex modulus is decomposed into storage (G′(ω)) and loss parts (G′′(ω)) by applying a corresponding phase angle and by using the Fourier transformation with the prony parameters as shown in Equations 4 & 5**.** A Nonlinear least square regression method is used to fit both components and to determine the Prony series parameters (Tzikang, 2000).

$$G'(\omega) = G_0\left(1-\sum_{i=1}^{N} g_i\right) + G_0\sum_{i=1}^{N}\frac{g_i\tau_i^2\omega^2}{1+\tau_i^2\omega^2} = |G^*|\cos(\phi) \tag{4}$$

$$G''(\omega) = G_0\sum_{i=1}^{N}\frac{g_i\tau_i\omega}{1+\tau_i^2\omega^2} = |G^*(\omega)|\sin(\phi) \tag{5}$$

where the angular frequency ω= 2πf and ϕ is phase angle obtained from Dynamic Modulus test. For the current paper the HMA material properties are adopted from the work of Baek (2010). Table 1 shows the values of prony series parameter used for the HMA at -10°C.

Table 1. Prony series parameters for HMA (Baek, 2010)

N		1	2	3	4	5	6	7	8	9
g_i		0.07	0.096	0.114	0.136	0.119	0.11	0.1	0.083	0.06
k_i		0.07	0.096	0.114	0.136	0.119	0.11	0.1	0.083	0.06
τ_i		10^{-4}	10^{-3}	0.01	0.1	1	10	100	10^3	10^4
E_0		17.2 GPa								
μ		0.2								

2.2 Fracture Properties for modelling crack initiation and propagation.

A clear finite element algorithm for modelling crack propagation was developed in 1999 based on partition of unity method, i.e. sum of shape functions must be unity, described as eXtended Finite Element Method (XFEM) (Belytschko, and Black, 1999). By this method, a crack arbitrarily aligned within the mesh can be represented by means of enrichment functions. This method avoids re-meshing and the stress intensity factors can be computed with errors less than 1 percent. Using the partition of unity method, XFEM adds a priori knowledge about the solution and makes it possible to model the discontinuities and singularities independent of the mesh. This makes it a very attractive method to simulate crack propagation since it is not necessary to update the mesh to match the current geometry of the discontinuity and the crack can propagate in a solution-dependent path. While modelling the crack propagation, singularity at the crack tip and discontinuities in the displacement field should be taken care. In XFEM, enrichment functions connected to additional degrees of freedom are added to the finite element approximation. These enrichment functions consist of the asymptotic crack tip functions that capture the singularity at the crack tip and a discontinuous function that describes the gap between the crack surfaces (Heaviside Functions). With the aid of Figure 2, the formulation of XFEM for crack propagation is expressed. All the nodes in the mesh are defined by a set S, the nodes surrounding the crack tip by S_c and the nodes whose elements are cut by crack are defined as S_h (Excluding the nodes in S_c).

Finite element algorithm for these enrichment functions is written in the FE software ABAQUS 6.12-3 based on the approximation as shown in Equation 6.

$$u = \sum_{I \in S} \left[u_I + \underbrace{H(x) a_I}_{I \in S_h} + \underbrace{\sum_{i=1}^{4} \psi_i(x) b_I^i}_{I \in S_c} \right] \tag{6}$$

where, u_I is the nodal displacement vector, a_I is the nodal enriched degree of freedom vector that with the jump function $H(x)$ and b_I^i is the nodal enriched degree of freedom vector that with the crack tip functions $\psi_i(x)$ which represent the crack tip singularity.
The main advantage of this method is that the crack path is solution dependent and no need of re-meshing. Toolabi et al. (2013) have proven that XFEM can be used for linear viscoelastic materials by analysing a 2-D cracked body made of a viscoelastic orthotropic body. The values of stress intensity factors obtained from XFEM and conventional FEM are found to be comparable. Sebnem, and Cagri (2014) have modelled crack propagation using FEM, CZM and XFEM in a linear viscoelastic material. It has been proven that, XFEM is more suitable for bulk material crack propagation where the crack path is not known a priori. Definition of fracture properties in XFEM is very similar to the definition of fracture definition in CZM. The only difference is, there is no need of initial modulus in XFEM which is essential in CZM to avoid the compliance issues due to insertion of cohesive elements. Based on the observation the fracture properties for the current model is taken from the results of Disk shape compact tension test (DCT). The area under the graph plotted between the load and CMOD shows the fracture energy. No test was performed to calculate the cohesive strength of the material. It was

calculated based on the elastic theory in accordance with ASTM E399, from the peak load in load-CMOD curve. Initial Modulus for CZM is given to avoid the compliance caused due to insertion of cohesive elements in the FE model. The fracture properties are given in Table 2.

Table 2. Fracture properties of HMA (Baek, 2010) and Interface properties of Control specimen, Coir, Jute and Synthetic Geotextile

Property	HMA Value	Control Specimen	Coir GT	Jute GT	Synthetic GT
Cohesive Strength (MPa)	2.55	1.35	0.47	1.13	1.14
Fracture energy (J/m^2)	220	2680	800	980	1100
Initial modulus (CZM) (MPa)	17200	1100	256	525	650

2.3 Modelling of interface

Interface between HMA layer and geosynthetic material plays a vital role in the numerical modelling. The interactions along an interface can be modelled by introducing suitable elements along this interface. Goodman et al. (1968) were the first to introduce zero thickness interface elements. Unlike continuum elements, stresses in the interface elements are calculated from the shear and normal displacements. In ABAQUS, interface is modelled using cohesive elements. Constitutive behaviour of these cohesive elements is defined using Traction Separation Law. The initial slope represents the stiffness of cohesive elements. Once the shear or normal stress reaches the corresponding ultimate strength, stiffness starts degrading according to the given damage evolution criteria (Simulia, 2013).

Therefore, in the present study, crack propagation is modelled using XFEM and interface is modelled using cohesive elements. Researchers have found that there is good agreement between these two methods. Mubashar et al. (2014) have proven that, the XFEM and CZM can be used together for modelling crack propagation and interface between two dissimilar materials respectively.

Leutner shear test is one of the easy and reliable method for the measurement of the strength along the HMA-geosynthetic interface (Sudarsanan et al., 2016). The test is conducted at a strain rate of 50 mm/min and at a constant temperature of -10°C. The sample is of the size of diameter 150 mm and 100 mm in height. Figure 3 shows the test setup for the Leutner shear test. Based on the shear stress vs strain plot the main parameters required to define the interface model are shear and normal stiffness, ultimate strength or cohesive strength and fracture energy. The measured parameters are shown in Table 2.

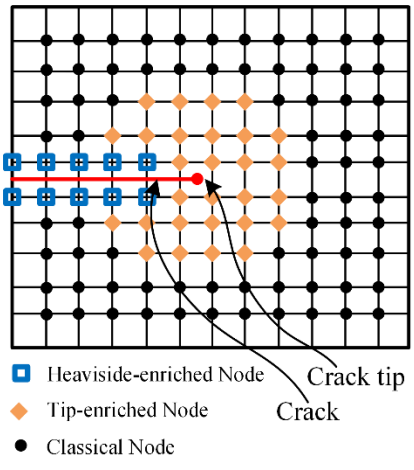

Figure 2. The arbitrary crack in XFEM

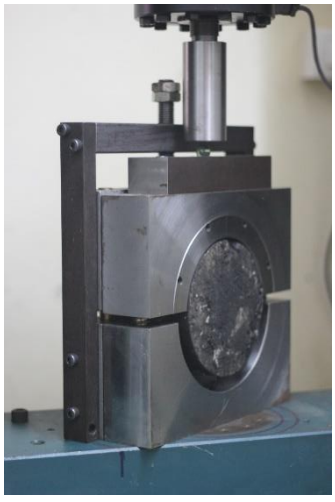

Figure 3. Leutner Shear test setup

3. VALIDATION OF MATERIAL ROPERTIES

3.1 Asphalt Concrete

Time dependent visco-elastic behavior of the HMA is validated by modelling the Indirect tensile test (IDT) used to predict the creep behavior. The dimension of the cylindrical sample is of diameter 150 mm and 39.8 mm thickness and a loading steel plate of dimensions 39.8 mm × 10 mm × 10 mm are created. In this model, the instances are assembled similar to the experimental setup shown in Figure 4. The material model for the HMA is defined as linear visco-elastic material and steel is defined as linear elastic. Prony parameters are used to define the linear visco-eleastic behavior as explained in section 2.1. Linear elastic behavior is defined using elastic modulus and Poisson's ratio. A concentrated load of 2 kN is applied on the top steel plate. Boundary conditions are given to ensure that there is no rigid body motion in the analysis and mimic the real laboratory conditions. Bottom steel plate is constrained in all the three directions using displacement boundary condition. Moreover, tie constraints are given between the steel plates and corresponding nodes on the cylindrical specimen to ensure a firm bond between them.

The model is meshed by sweeping technique along the thickness of the cylindrical specimen with an 8 noded brick elements (C3D8). The same meshing is done on steel plate as well. The generated mesh is shown in Figure 4. For this particular model, Horizontal and vertical displacements are measured between two points separated by a gauge distance of 38.1 mm at the center of specimen in each direction. The comparison of obtained results shows good agreement with the experimental result measured by Baek (2010) (Figure 5**)**.

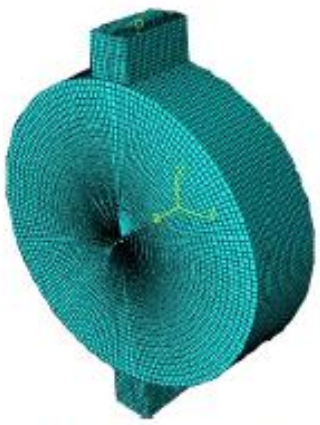

Figure 4. 3D mesh of IDT setup

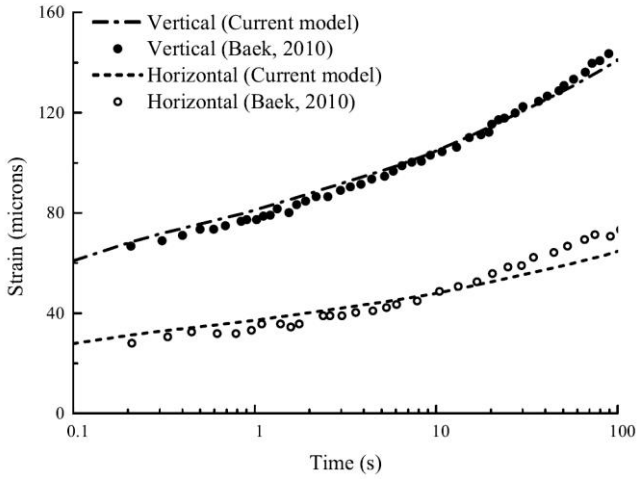

Figure 5. Validation of HMA material properties

4. VALIDATION OF CRACK PROPAGATION MECHANISM

Accuracy of numerical modelling of crack propagation depends on the method adopted for modelling it. ABAQUS contains finite element algorithm for both Cohesic Zone Modelling (CZM) and eXtended Finite Element Method (XFEM). Baek (2010) has conducted experiment and modelled crack propagation using CZM in Disk Shape Compact tension test. The same test is recreated with a difference that the crack is modelled using recent XFEM algorithm to check the applicability of this method.

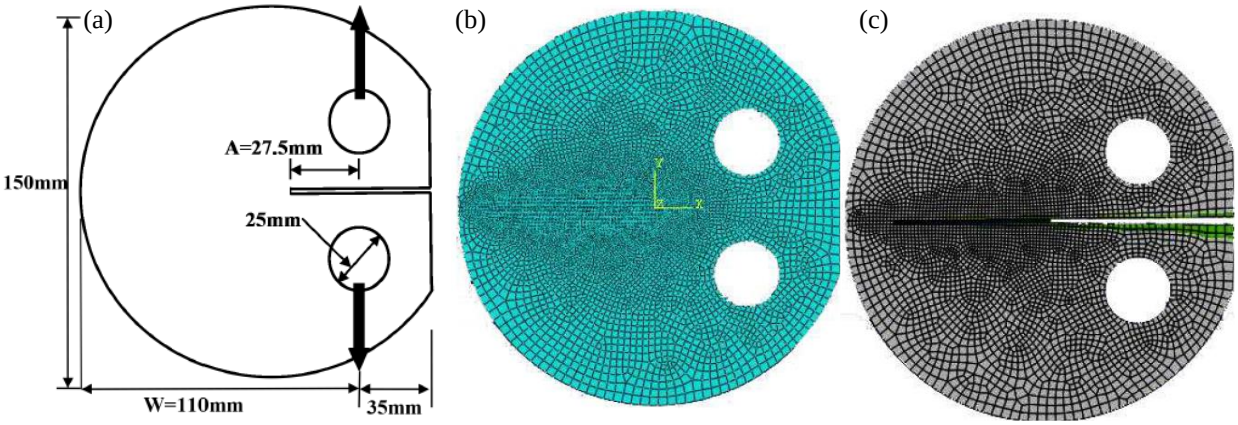

Figure 6. (a) Schematic diagram of DCT test setup (b) Generated mesh for DCT test setup using XFEM (c) Crack path observed in DCT using XFEM

A 2D Geometry of DCT test setup is created as per the dimensions shown in Figure 6(a). Main advantage of this method is that the crack path is solution dependent, so there is no need to define the crack path prior to the analysis as it is done in CZM. Definition of fracture properties in XFEM is very similar to the definition of fracture definition in CZM. The only difference is, there is no need of initial modulus in XFEM which is essential in CZM to avoid the compliance issues due to insertion of cohesive elements. In addition to the four damage initiation criteria for CZM model, two more initiation criteria are available for XFEM which are maximum principal stress criterion (MAXPS) and maximum principal strain criterion (MAXPE). In MAXPS & MAXPE, maximum value of principal stress and maximum value of principal strain at the time of damage initiation should be given respectively. In the present model, MAXPS is given as damage initiation criterion and cohesive strength in Table 2 is given as maximum principal stress. Damage evolution criterion is defined very similar to the damage evolution criterion in CZM. A viscosity coefficient of 0.0001 is given to avoid the convergence issues. After the material properties are created, a homogeneous section with out of plane thickness of 40mm is created. Step time for this particular step is mentioned as 120sec. Velocity boundary conditions are given to simulate a tensile load at a constant strain rate of 0.8 mm/min at the holes.

Initial crack in XFEM is defined in interaction module unlike CZM. In present model, as the geometry is small whole cross section is chosen as enrichment region. One more interaction property is given specifying the relation between two crack surfaces when they are getting separated. This interaction property includes elastic modulus of the main material (Simulia,

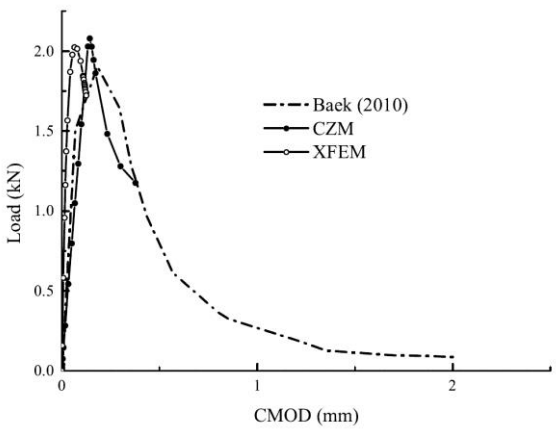

Figure 7. Comparison of results of CZM and XFEM with literature

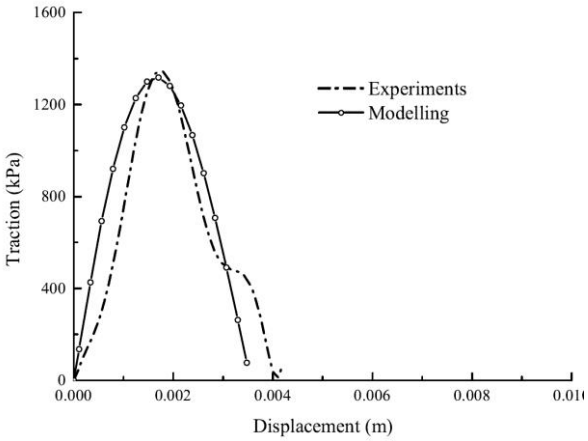

Figure 8. Comparison of Interface modelling with Leutner shear test results

2013). Asphalt concrete is assigned with 4 noded bilinear plane stress quadrilateral elements. Mesh is made finer in the vicinity of expected crack as shown in Figure 6(b), (c). Considering the above results shown in Figure 7, it has been concluded that XFEM can be used for further analysis.

5. VALIDATION OF INTERFACE PROPERTIES

A 3 dimensional cylindrical sample of dimensions 150 mm diameter and 100 mm height is created. Interface is present at 50 mm depth. This interface is modelled using cohesive elements and these cohesive elements are given negligible thickness 0.1mm. Bottom half of the cylinder is completely fixed and shear load is applied on the top half at a constant strain rate of 50 mm/min using velocity boundary conditions. Here, bottom and top faces of cohesive layers are tied to top face of bottom part and bottom face of top part respectively. Asphalt concrete is meshed using 8 node brick elements (C3D8) and the interface elements using 8 node three dimensional cohesive elements (COH3D8). Stacking direction of cohesive elements is given along the Z-direction. The result shown in Figure 8 proves that the adopted method for interface modelling is valid and the same method is applied in further analysis.

6. MODELLING OF THREE POINT BEAM BENDING

Efficiency of interface layers is checked by comparing the results of numerical modelling of Three-point beam bending test (TPB) with and without interface layers. A 2-dimensional beam of length 400 mm and depth 100 mm is created. Out of plane thickness is given as 100 mm. There is an initial crack at the bottom middle of the beam and the length of crack is 15 mm. Loading and boundary conditions are given similar to actual loading conditions in laboratory. Two roller supports are placed at a distance of 50 mm from both the sides. A constant strain rate of 6.25 mm/min is applied at the top midpoint of the beam. 4 noded bilinear plane stress quadrilateral elements (CPS4) and 4-node two dimensional cohesive elements are given for HMA and interface layer respectively. Figure 9 shows the results and the crack pattern obtained for TPB without reinforcement. In the case of reinforced samples, geosynthetic layer is created with same length of the beam and it has a base feature of shape wire and planar type (two dimensional). 2-node linear truss elements are used for geosynthetic material. Interface between these material is modelled using cohesive elements. 4 noded two dimensional cohesive elements (COH2D4) are used for interface layers between geosynthetic material and HMA. Figure 10 shows the assembly of beam with the inclusion of geosynthetic reinforcement.

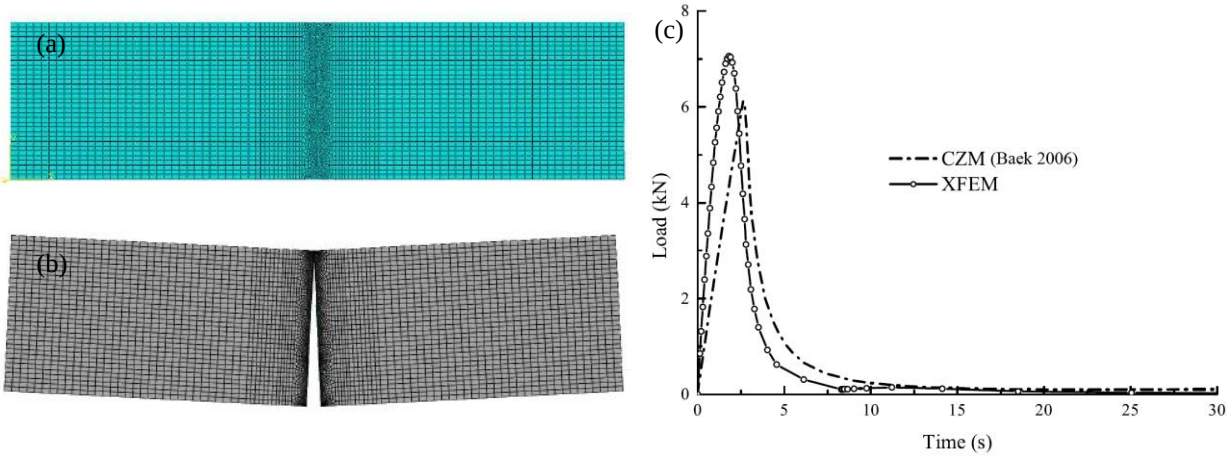

Figure 9. (a) Generated mesh in TPB model using XFEM, (b) Crack propagation path observed in TPB using XFEM, (c) Comparison of results of TPB modelling without interface using CZM and XFEM.

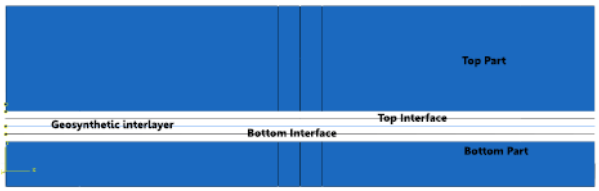

Figure 10. Arrangement of different parts in TPB model with interlayers

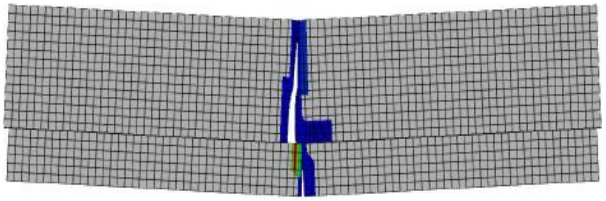

Figure 11. Propagated path in TPB with Coir as interlayer

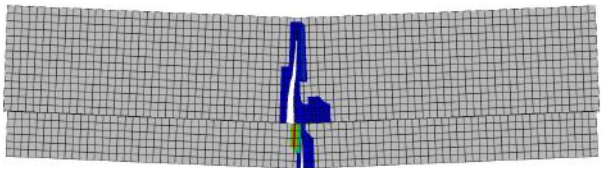

Figure 12. Propagated path in TPB with Jute as interlayer

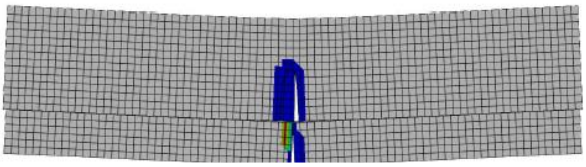

Figure 13. Propagated path in TPB with Synthetic material as interlayer

The results for the simulation of models are as show in Figure 14 (a), depicts that a significant improvement in the ultimate strength of the material can be possible due to the inclusion of the geotextile. Moreover, the time required for the crack to reach the top of the beam is delayed due to the inclusion of the reinforcement and the stress near the crack is distributed at the geosynthetic – HMA interface as show in Figure 11, 12, 13. Figure 14(b) describes the trend of stresses developed in the interface under the three-point loading and shows that the material fails at the point when the products ultimate capacity reaches.

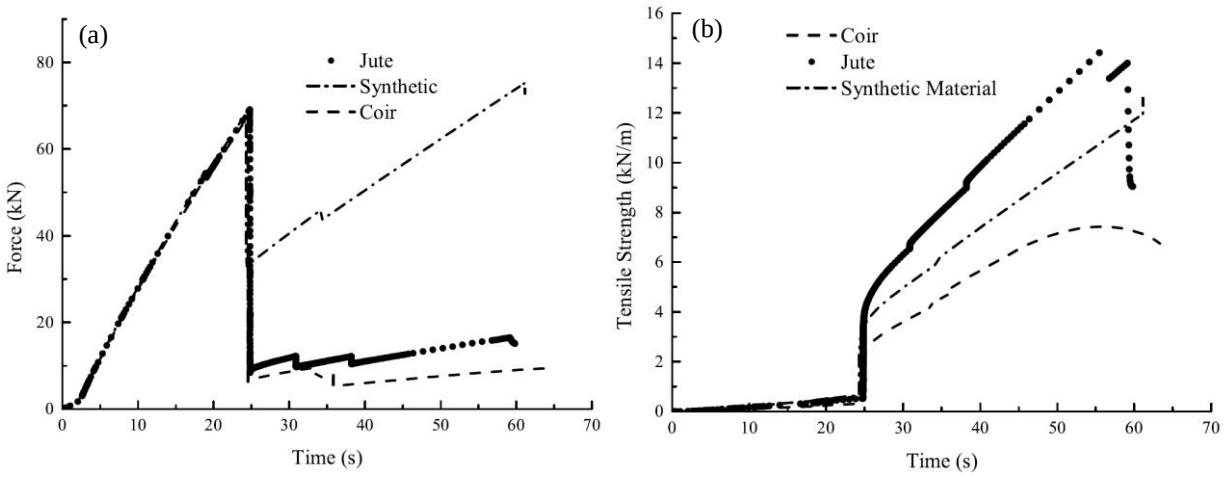

Figure 14. (a) Reaction force generated in TPB test with three interlayers (b) Tensile stresses developed in different synthetic materials.

7. CONCLUSIONS

Mechanism that is chosen for analysing crack initiation and crack propagation plays an important role in predicting the material behavior. The results obtained from CZM and XFEM are compared with the results of Baek (2010), and XFEM results are found to give almost the same. The solution dependent crack path is the greater advantage of XFEM in spite of the convergence difficulties which can be nullified if proper care is taken while meshing the model. The observed results of numerical simulations of Leutner shear test says that defining interface between two surfaces using cohesive elements of negligible thickness with traction separation response is an efficient way of representation. Numerical modelling of three-point beam bending test without interlayers has shown that, HMA at a temperature of -10°C is brittle as

the complete failure occurs within 10 sec from the beginning of loading. From the obtained results, it can be said that the inclusion of geosynthetic materials are fulfilling their requirement of absorbing tensile stresses. It has been also found that time taken by the crack to reach the top surface is increased with geosynthetic inclusions.

REFERENCES

A. Khodaii, S. Fallah and F.M. Nejad (2009) Effects of geosynthetics on reduction of reflection cracking in asphalt overlays, *Geotextiles and Geomembranes*, 27, No. 1, 1-8.

A. Mubashar, I. Ashcroft and A. Crocombe (2014) Modelling Damage and Failure in Adhesive Joints Using A Combined XFEM-Cohesive Element Methodology, *The Journal of Adhesion*, 90, No. 8, 682-697.

A.H. De Bondt (1999) *Anti-reflective cracking design of (reinforced) asphaltic overlays*. TU Delft, Delft University of Technology, Delft, Netherlands.

C. Tzikang, Determining a Prony series for a viscoelastic material from time varying strain data. (2000) *NASA Langley Research Center, U.S. Army Research Laboratory.* Hampton, Virginia, USA. NASA / TM-2000-210123, 21.

D. Simulia (2013) *ABAQUS 6.13 User's Manual*, Dassault Systems, Rising Sun Mills, 166 Valley Street, Providence, RI, USA.

J. Baek (2010) *Modeling reflective cracking development in hot-mix asphalt overlays and quantification of control techniques*. Dissertation, University of Illinois at Urbana-Champaign, IL, United States.

J. Baek and I.L. Al-Qadi (2006) Finite element method modeling of reflective cracking initiation and propagation - Investigation of the effect of steel reinforcement interlayer on retarding reflective cracking in hot-mix asphalt overlay, *Pavement Rehabilitation, Strength and Deformation Characteristics, and Surface Properties-Vehicle Interaction 2006*, No. 1949, 32-42.

J.W. Button and R.L. Lytton (2007) Guidelines for using geosynthetics with hot-mix asphalt overlays to reduce reflective cracking, *Transportation Research Record*, No. 2004, 111-119.

M. Toolabi, A.S. Fallah, P.M. Baiz and L.A. Louca (2013) Dynamic analysis of a viscoelastic orthotropic cracked body using the extended finite element method, *Engineering Fracture Mechanics*, 109, 17-32.

N. Sudarsanan, R. Karpurapu and V. Amrithalingam (2016) Critical review on the bond strength of geosynthetic interlayer systems in asphalt overlays, *Japanese Geotechnical Society Special Publication*, 2, No. 67, 2296-2301.

Ö. Sebnem and I. Cagri (2014) Modeling Cracks in Nonlinear Viscoelastic Media Subjected to Thermal Loading, *50th AIAA/ASME/SAE/ASEE Joint Propulsion Conference*, American Institute of Aeronautics and Astronautics, Cleveland, Ohio, USA.

R. Christensen (2012) *Theory of Viscoelasticity: An Introduction*, 2 ed., Elsevier Science, New York, USA.

R.E. Goodman, R.L. Taylor and T.L. Brekke (1968) A model for the mechanics of jointed rock, *Journal of Soil Mechanics & Foundations Div*, 94, 637-659.

S. Nithin, K. Rajagopal and A. Veeraragavan (2014) Reflection cracking: a review on the potential of interlayer system with reference to natural fibres, *10th international conference on geosynthetics*, German Geotechnical Society, Berlin, Germany.

S. Nithin, K. Rajagopal and A. Veeraragavan (2015) State-of-the Art Summary of Geosynthetic Interlayer Systems for Retarding the Reflective Cracking, *Indian Geotechnical Journal*, 45, No. 4, 472-487.

T. Belytschko and T. Black (1999) Elastic crack growth in finite elements with minimal remeshing, *International Journal for Numerical Methods in Engineering*, 45, No. 5, 601-620.

T.A. Bennert (2009) *A rational approach to the prediction of reflective cracking in bituminous overlays for concrete pavements*. Dissertion, Rutgers, The State University of New Jersey, New Jersey, USA.

Y.R. Kim (2009) *Modeling of asphalt concrete*, ASCE Press, McGraw-Hill, Reston, VA, New York.